nature neuroscience

Traveling waves in developing cerebellar cortex mediated by asymmetrical Purkinje cell connectivity

Alanna J Watt[1], Hermann Cuntz[1], Masahiro Mori[1,2], Zoltan Nusser[3], P Jesper Sjöström[1] & Michael Häusser[1]

Correlated network activity is important in the development of many neural circuits. Purkinje cells are among the first neurons to populate the cerebellar cortex, where they sprout exuberant axon collaterals. We used multiple patch-clamp recordings targeted with two-photon microscopy to characterize monosynaptic connections between the Purkinje cells of juvenile mice. We found that Purkinje cell axon collaterals projected asymmetrically in the sagittal plane, directed away from the lobule apex. On the basis of our anatomical and physiological characterization of this connection, we constructed a network model that robustly generated waves of activity that traveled along chains of connected Purkinje cells. Consistent with the model, we observed traveling waves of activity in Purkinje cells in sagittal slices from young mice that require $GABA_A$ receptor–mediated transmission and intact Purkinje cell axon collaterals. These traveling waves are absent in adult mice, suggesting they have a developmental role in wiring the cerebellar cortical microcircuit.

The cerebellar cortex is one of the best-characterized circuits of the CNS and is important in the precise timing of motor control[1]. Purkinje cells form the sole output of the cerebellar cortex and project to the deep nuclei of the cerebellum (DCN), where they form GABAergic synapses. Purkinje cells also have local axon collaterals, which typically bifurcate in the granule cell layer and project back up to the Purkinje cell layer and occasionally into the molecular layer[2]. The synaptic target(s) and function of the Purkinje cell local axon collaterals have long been the subject of controversy, although some studies since the pioneering work of Cajal have suggested that they form synapses onto other Purkinje cells[2–4] (but see refs. 5,6). Direct evidence for functional synaptic connections between Purkinje cells has only recently been described[7]. Because this local recurrent pathway is generated by the output neurons of the network, it is probably important in controlling activity patterns of the cerebellar cortex. Indeed, a recent modeling study suggested that Purkinje-Purkinje connections could both enhance temporal integration and synchronize neurons in the cerebellar cortex[8].

Given that Purkinje cells are among the earliest neurons to migrate into the cerebellar cortex (as early as embryonic day 15)[9], they are in the right place at the right time to orchestrate the development of the synaptic connections in the cerebellar cortex. It has recently been demonstrated that the axon collaterals of juvenile Purkinje cells are particularly exuberant and are pruned to a mature distribution by the third week of postnatal development[10]. This suggests that Purkinje-Purkinje synapses may be particularly important during early stages of development, at a time when basket and stellate cell synaptic inputs onto Purkinje cells have not yet been established[11].

In several CNS regions, including the visual system, the hippocampus and the spinal cord, spontaneous traveling waves of activity early in development are critical for establishing the accurate synaptic connectivity of mature circuits[12–14]. However, wave-like activity has not previously been described in the developing cerebellum. To investigate the properties of monosynaptic connections between Purkinje cells and to probe their contribution to network activity in cerebellar cortex, we used two-photon laser scanning microscopy to guide targeted patch-clamp recordings from connected pairs in slices from transgenic mice expressing green fluorescent protein (GFP) in Purkinje cells. We found that the asymmetrically projecting Purkinje-Purkinje synaptic connections provide a robust substrate for propagating waves of activity in the developing, but not adult, cerebellum.

RESULTS

Functional synapses between juvenile Purkinje cells

To study the synaptic targets of Purkinje cell axon collaterals, we used transgenic mice that express the fusion protein tau-GFP under the control of the Purkinje cell–specific *L7* (also known as *Pcp2*) promoter[15]. In these mice, the tau component of the chimera results in GFP enrichment in axons[15]. Because the *L7* promoter specifically drives expression in Purkinje cells, we were able to use GFP as a marker for Purkinje cell axon collaterals. To maximize the chance of obtaining synaptically connected pairs, we made targeted patch-clamp recordings from putatively connected pairs that were visualized using a custom-designed two-photon laser-scanning microscope in juvenile slices from *L7–tau* (also known as *Mapt*)*-gfp* transgenic mice or, in a few cases, *Gad65* (also known as *Gad2*)*-egfp* mice[16,17]. We visualized individual Purkinje cell axon collaterals and traced them to their putative postsynaptic targets (**Fig. 1a**; see Methods), which were also visualized simultaneously using laser-scanning Dodt contrast imaging. We then

[1]Wolfson Institute for Biomedical Research and Department of Neuroscience, Physiology and Pharmacology, University College London, London, UK. [2]Department of Physiology and Biological Information, Dokkyo Medical University, Shimotsuga-gun, Tochigi, Japan. [3]Laboratory of Cellular Neurophysiology, Institute of Experimental Medicine, Hungarian Academy of Sciences, Budapest, Hungary. Correspondence should be addressed to A.J.W. (a.watt@ucl.ac.uk).

Received 11 August 2008; accepted 27 January 2009; published online 15 March 2009; doi:10.1038/nn.2285

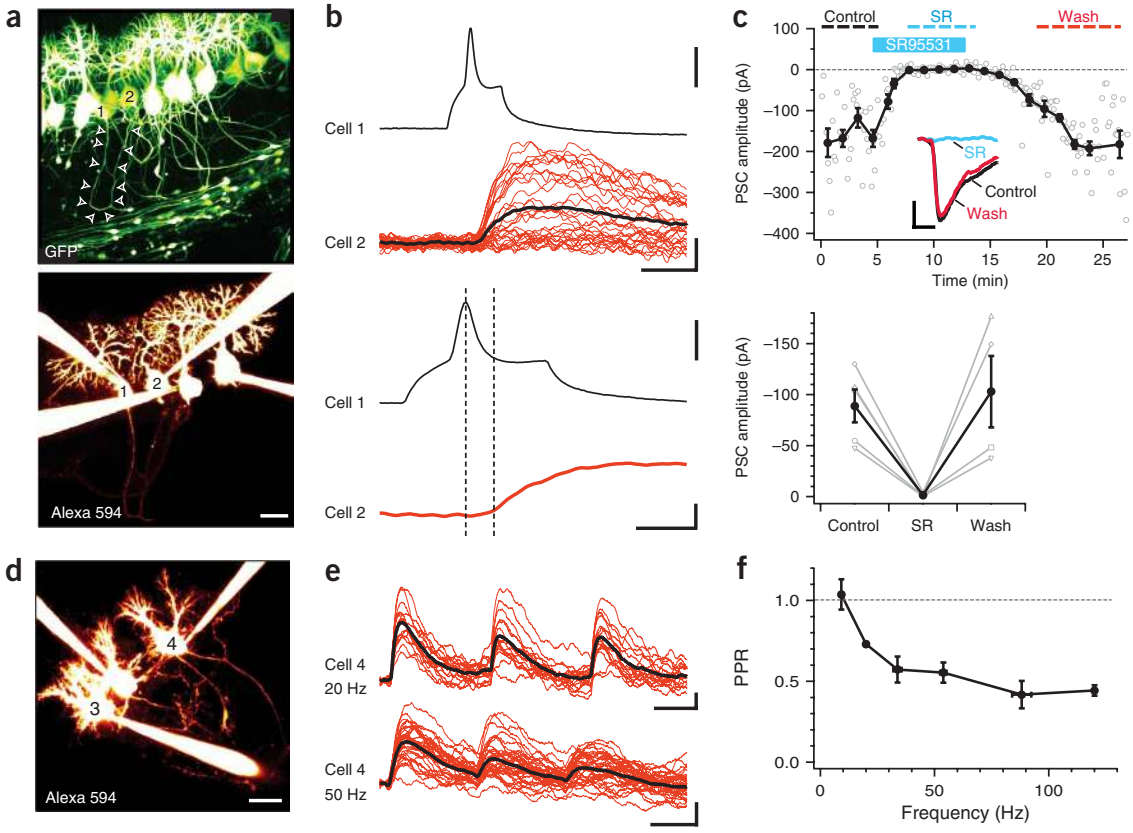

Figure 1 Unitary synaptic connections between neighboring Purkinje cells. (**a**) Top, two-photon image of Purkinje cells from a P9 *L7-tau-gfp* mouse. Bottom, quadruple whole-cell recordings of Purkinje cells selected from the GFP image above, imaged with Alexa 594 in the internal solution. A synaptic connection was found between cells 1 and 2. Scale bar represents 20 μm. (**b**) Unitary synaptic connection between Purkinje cells. Top, a spike in cell 1 evoked a PSP in cell 2 (red, individual responses; black, average response; $V_{hold} = -80$ mV, with symmetrical chloride internal solution). Scale bars represent 25 mV (top), 2 mV (bottom) and 5 ms. Bottom, the same connection is shown, expanded to illustrate the latency. Scale bars represent 25 mV (top), 1 mV (bottom) and 2 ms. (**c**) Top, sample experiment showing that synaptic currents were reversibly blocked by SR95531 (SR; open circles = individual responses; filled circles = 2-min averages). Inset, superimposed average PSCs (times indicated by the dashed lines). Scale bars represent 50 pA and 4 ms. Bottom, summary data (gray symbols, individual experiments; black symbols, mean ± s.e.m.; $n = 5$ for control and SR95531, $n = 4$ for wash). (**d**) Recording configuration in **e**. Cell 3 was presynaptic to cell 4. Scale bar represents 20 μm. (**e**) Responses in cell 4 to 20 Hz (top) and 50 Hz (bottom) spike trains in cell 3 showed short-term depression (red, individual responses; black, averages). Scale bars represent 0.5 ms and 20 ms above, and 0.5 ms and 10 ms below. (**f**) PPR varied with presynaptic firing frequency (3–13 data points per bin, $n = 20$ connections). All error bars represent ± s.e.m.

made simultaneous triple or quadruple whole-cell recordings from candidate pre- and postsynaptic neurons. To confirm the identity of the neurons (**Fig. 1a**), Alexa 594 and biocytin were included in the internal solution, permitting the imaging and subsequent reconstruction of the neurons (see below). Purkinje cells were hyperpolarized with constant direct current injection (presynaptic $V_m = -69.1 \pm 2.1$ mV, postsynaptic $V_m = -74.6 \pm 2.3$ mV, $n = 20$) to prevent spontaneous spiking and brief current pulses were injected to elicit spikes to test for connections. Synaptic connections between pairs of Purkinje cells were observed in 26% of attempts (or 23 pairs out of 88 tested, postnatal days 4–14 (P4–14)). This was a 20-fold improvement on the nontargeted connectivity rate, which was 1.3% (2 pairs out of 154 tested).

The Purkinje-Purkinje cell synaptic connections (**Fig. 1b**) were depolarizing in our recordings because of the symmetrical chloride internal solution that we used to maximize synaptic driving force and thus the signal-to-noise ratio. The postsynaptic responses had short latencies and little temporal jitter (latency = 0.60 ± 0.05 ms, $n = 20$; **Fig. 1b** and **Supplementary Table 1** online), consistent with monosynaptic connections. The mean postsynaptic potential (PSP) rise time was 2.2 ± 0.24 ms ($n = 20$), with a τ_{decay} of 20 ± 1.9 ms ($n = 17$; **Supplementary Table 1**). The mean peak amplitude of connected pairs was 1.9 ± 0.63 mV ($n = 14$, including failures), with a high degree of variability across connections (**Supplementary Table 1**). The trial-to-trial variability in PSP amplitude was also considerable, with a coefficient of variation (s.d. divided by the mean) of 0.9 ± 0.13 ($n = 20$; **Supplementary Table 1**). Consistent with the large range of coefficient of variations, the failure rates were also variable (**Supplementary Table 1**). Synaptic currents measured in voltage clamp showed relatively rapid kinetics (rise time = 0.8 ± 0.13 ms, $\tau_{decay} = 5.8 \pm 0.99$ ms, $n = 11$; **Supplementary Table 1**), consistent with a perisomatic location of the synaptic contacts. Although the Purkinje-Purkinje synaptic properties were characterized over an age range during which the cerebellar circuit changes markedly (P4–14), when comparing data from mice in the P4–6 and P7–14 age groups, we found no significant differences in PSP amplitude ($n = 7$ out of 7 P4–6/P7–14, $P = 0.90$), latency ($n = 9$ out of 12, $P = 0.89$) or τ_{decay} ($n = 9$ out of 12, $P = 0.63$), which allowed us to pool the data from these two age groups (**Supplementary Fig. 1** online). We applied the selective $GABA_A$ receptor antagonist SR95531 to investigate the receptors underlying the synaptic connection between Purkinje cells. SR95531 completely and reversibly abolished synaptic responses (**Fig. 1c**), indicating that these synapses are GABAergic.

We next investigated the short-term plasticity of the Purkinje-Purkinje cell synapses with presynaptic spike trains and measured the paired-pulse ratio (PPR) of the responses (see Methods; **Fig. 1d–f**).

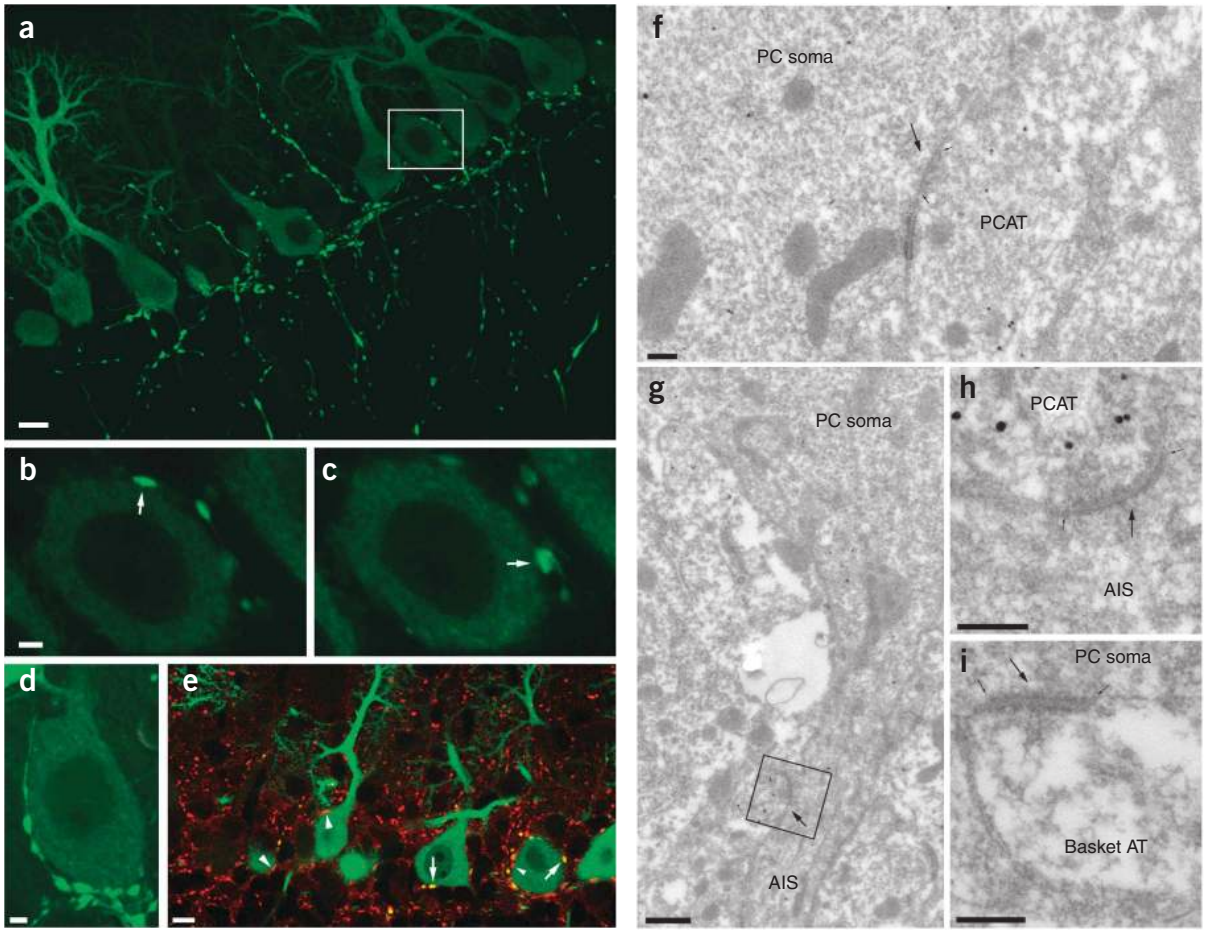

Figure 2 Purkinje cell local axon collaterals establish synapses on other Purkinje cells. (**a**) Confocal laser scanning microscopic image of the cerebellar cortex of an *L7-tau-gfp* mouse. Scale bar represents 10 μm. (**b**,**c**) High-magnification single optical section images from the boxed area in **a**. Arrows indicate the site of potential synaptic interactions. Scale bar represents 2 μm. (**d**) A single Purkinje cell soma could be surrounded by a large number of Purkinje cell axon terminals. (Fluorescent image is superimposed on a differential interference contrast image). Scale bar represents 2 μm. (**e**) Double immunofluorescence labeling for GFP (green) and VIAAT (red) indicated that GFP-containing Purkinje cell axon varicosities (arrows) were VIAAT-positive (yellow). Some VIAAT-positive, but GFP-negative, boutons (arrowheads) also contacted Purkinje cell somata. Scale bar represents 5 μm. (**f**) An electron micrograph showing a Purkinje cell axon terminal (PCAT) establishing a synaptic junction (arrow) with a Purkinje cell (PC) soma. The presence of gold particles indicates immunoreactivity for GFP. For illustrative purposes, the edges of the synaptic junction are marked with small arrows. Scale bar represents 0.2 μm. (**g**,**h**) An axon initial segment (AIS) emerging from a Purkinje cell soma received a synapse (arrow) from a GFP-positive axon terminal (PCAT; **g**). The boxed area in **g** is shown at a higher magnification in **h**. Scale bars represent 0.5 μm (**g**) and 0.2 μm (**h**). (**i**) Purkinje cell somata also received synapses (arrow) from GFP-negative boutons, which probably originate from basket cells (Basket AT). Scale bar represents 0.2 μm.

Paired-pulse depression was observed at frequencies above 10 Hz (**Fig. 1f**), with increasing depression at higher frequencies, which reached a plateau of ~40% at ~90 Hz. Paired-pulse depression was developmentally regulated; it was strong in the first postnatal week (P4–6, PPR = 0.49 ± 0.06) and was significantly reduced in the second week (P7–14, 0.97 ± 0.15, $P = 0.009$; **Supplementary Fig. 1**). In summary, synaptic connections between young Purkinje cells are GABAergic and show short-term synaptic depression and high trial-to-trial and cell-to-cell variability in the amplitude and reliability of the response.

Ultrastructure of synapses between Purkinje cells

We further studied the distribution of synaptic contacts between Purkinje cells using immunolabeling at both light microscopic and electron microscopic levels. Confocal imaging (**Fig. 2a**) showed that Purkinje cell axons formed presynaptic varicosities that were often directly apposed to Purkinje cell somata (**Fig. 2a–d**). To confirm that these varicosities were axon terminals containing vesicles, we carried out double immunolabeling for vesicular inhibitory amino acid transporter (VIAAT) and GFP (**Fig. 2e**). These two markers showed a colocalization in many varicosities that were seemingly in direct contact with Purkinje cell somata (**Fig. 2e**).

To investigate further, we examined these varicosities at the ultrastructural level by carrying out electron microscopic immunogold labeling of GFP. Our electron microscopy analysis confirmed the existence of symmetrical synaptic junctions made by GFP-positive axon terminals onto GFP-positive somata (**Fig. 2f**) and axon initial segments (AIS; **Fig. 2g**,**h**). We also found perisomatic synaptic junctions that were made by immunonegative axon terminals (**Fig. 2i**), which probably originated from basket cells that were beginning to innervate Purkinje cells at P8 (ref. 11). Taken together, our results indicate the existence of perisomatically located Purkinje-Purkinje cell synapses in juvenile cerebellum.

Anatomical organization of the Purkinje-Purkinje pathway

To help determine the effect of the Purkinje-Purkinje connection on the cerebellar cortical network, we examined the anatomical organization of

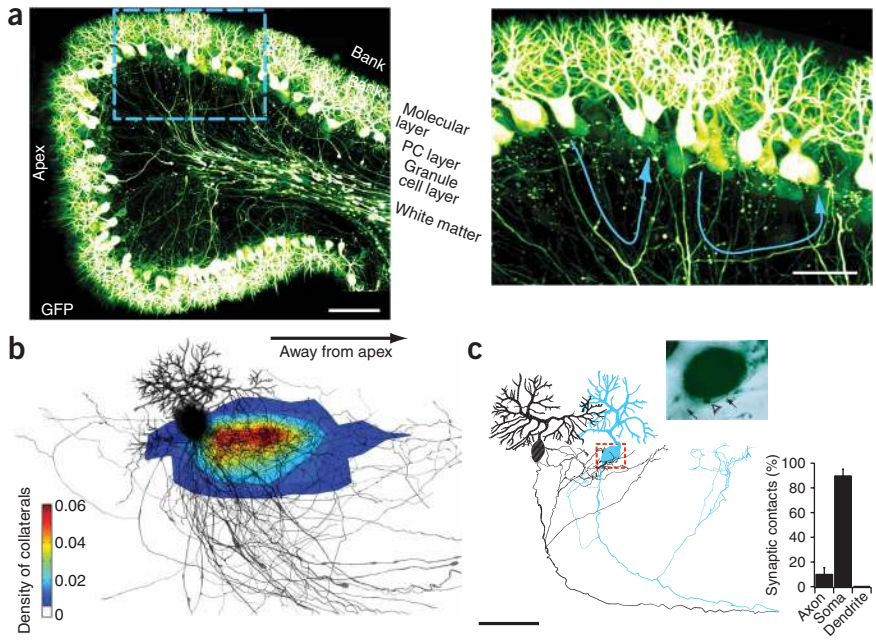

Figure 3 Anatomical distribution of Purkinje cell axon collaterals and Purkinje-Purkinje synapses. (**a**) Image of a lobule from a P9 mouse (left) and a high-magnification image of the region indicated by the blue dashed box (right) with two axon collaterals highlighted with blue arrows. Scale bars represent 100 μm and 50 μm (inset). (**b**) Density plot of Purkinje cell axon collaterals. Purkinje cell somata and axons (and some dendrites) were reconstructed and superimposed ($n = 39$; see Methods), and oriented with their axons projecting away from the apex of the lobule (left) and toward the DCN (right), as indicated. The density of collaterals (collateral cable length (μm) per area (μm^2)) is shown using a color scale, where red indicates highest density and blue lowest density. Scale bar represents 50 μm. (**c**) Neurolucida reconstruction of connected Purkinje cells (presynaptic cell, black; postsynaptic cell, blue) and a corresponding light microscopic single optical section (inset). The presynaptic axon (black arrows) made a putative presynaptic bouton onto the postsynaptic cell (white arrowhead). A summary of the subcellular location of putative synaptic contacts determined from biocytin-filled monosynaptically connected pairs is shown ($n = 7$ pairs). Scale bar represents 50 μm.

Purkinje cell collaterals following the reconstruction of the axons of biocytin-filled Purkinje cells. The main axon of Purkinje cells runs in the sagittal plane, projecting away from the tip (or apex) of a cerebellar lobule along the white matter toward the DCN[3]. Although there was considerable heterogeneity in the projection pattern of individual Purkinje cell axon collaterals (**Fig. 3a**), a motif emerged when a large number of collaterals were examined. We found a peak density of collaterals (and thus of postsynaptic partners) that was centered ~60 μm basally from the parent Purkinje cell, corresponding to ~1–5 Purkinje cell bodies (**Fig. 3b**). This argues that Purkinje-Purkinje cell connections are not randomly distributed in the cerebellar cortex, but instead form directed chains of connected cells in the sagittal plane. These chains begin at the apex of the cerebellar lobules and project basally (**Supplementary Movie 1** online). Because these data were obtained from cells lying at different locations in many lobules in the cerebellar vermis (**Supplementary Fig. 2** online), we suggest that this asymmetry may be a general feature of Purkinje axon collaterals. The anatomical asymmetry was confirmed in our functional connectivity data. In 20 out of 23 connected pairs (87%), the postsynaptic Purkinje cell was further away from the apex of the lobule than the presynaptic cell. In addition, although we always tested for reciprocal connections, we never observed one.

We were able to visually identify sites of putative synaptic contact at the light microscopic level in a subset of connected pairs ($n = 7$) that were digitally reconstructed. In most pairs, the presynaptic axon collateral branched substantially in the upper granule cell layer and Purkinje cell layer and then appeared to contact the postsynaptic Purkinje cell with several axon collaterals (**Fig. 3c**). In the majority of reconstructed pairs, the presynaptic axon collateral remained in the Purkinje cell layer without extending appreciably into the molecular layer, which implies that most synaptic contacts were not on dendrites. However, the occasional Purkinje cell collateral did enter the molecular layer (**Figs. 2a** and **3b**). On average, there were 3.7 ± 0.8 putative synaptic contacts made between each connected Purkinje cell pair ($n =$ 7 reconstructed pairs; **Supplementary Table 1**). Of these contacts, ~90% were made onto the soma and the remaining ~10% onto the AIS (**Fig. 3c**), consistent with our electron microscopic localization of Purkinje-Purkinje cell synapses (**Fig. 2g,h**) and with the rapid kinetics of PSC (**Supplementary Table 1**).

Entrainment of spiking by Purkinje-Purkinje synapses

Cerebellar Purkinje cells intrinsically generate regular spontaneous firing in the absence of synaptic input[18,19]. The effect of a synaptic input to a Purkinje cell can thus be measured by the extent to which it shifts the phase of spiking[20], rather than by the resulting membrane potential deflection at the soma. To assess the influence of Purkinje-Purkinje cell synaptic connections on Purkinje cell spiking, we used dynamic clamp circuitry to inject a conductance that mimicked this synaptic connection while allowing the postsynaptic cell to spike freely. Conductance kinetics and amplitude were determined on the basis of our paired recording data (**Supplementary Table 1** and **Supplementary Methods** online). Because the GABAergic reversal potential changed with development over the age range that we have studied[21] (**Supplementary Fig. 1**), we also benefited from the use of dynamic clamp, as it allowed us to vary the synaptic reversal potential while investigating the effect on postsynaptic spiking in the same Purkinje cell. As Purkinje-Purkinje synapses were primarily located perisomatically (**Figs. 2g,h** and **3c**), dynamic clamp with a somatic pipette accurately simulated this synaptic input (**Fig. 4a**).

When we injected a simulated depolarizing synaptic conductance in a freely spiking neuron (**Fig. 4b**), a structured firing pattern emerged in the postsynaptic cell. A similar, but opposite, effect was seen when the synaptic conductance was hyperpolarizing (**Fig. 4c**). As shown by cross-correlograms between spiking in the mock presynaptic neuron and the postsynaptic neuron for depolarizing (**Fig. 4b**) and hyperpolarizing reversal potentials (**Fig. 4c**), the simulated Purkinje cell connection entrained the postsynaptic cell.

We quantified the degree and the phase of entrainment by fitting sine waves to the cross-correlograms of pre- and postsynaptic spiking; the degree of entrainment was reflected by the sine wave amplitude and the phase (ϕ) by the location of the sinusoid peak. The degree of entrainment is smallest for reversal potentials around –50 mV, when inhibition is shunting[22]. Entrainment increased progressively in both directions from this point (**Fig. 4d**). The phase depended on the direction of the reversal potential deflection; depolarizing reversal potentials promoted relatively in-phase synchronization, whereas hyperpolarization favored anti-phase firing (**Fig. 4e**). Although the sign and magnitude of the change in average postsynaptic spiking

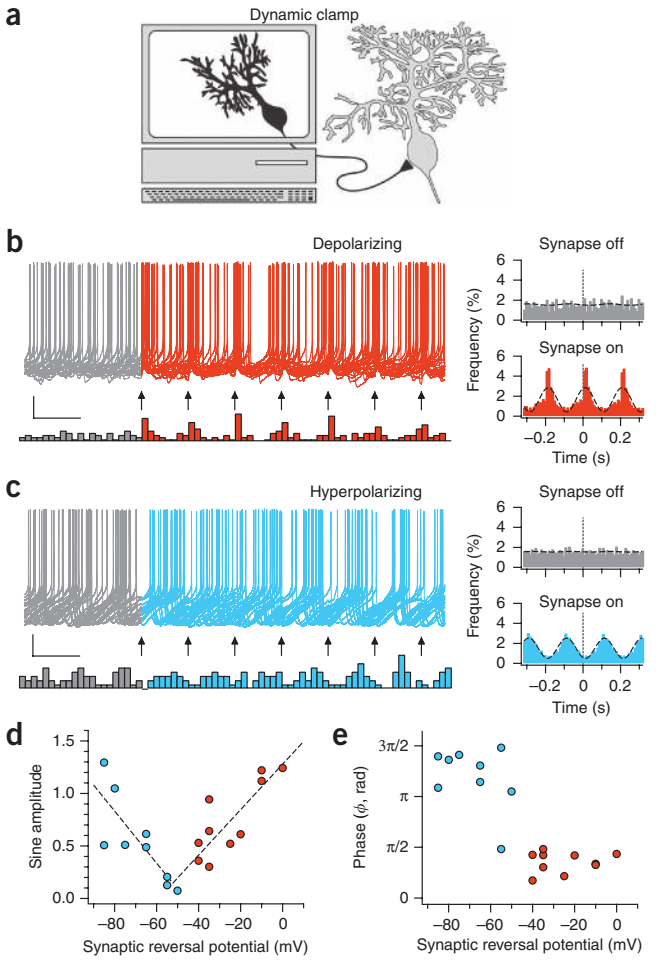

Figure 4 Purkinje cells synchronize in different phases depending on synaptic reversal potential. (**a**) Schematic illustration of recording configuration where a computer-generated dynamic clamp synaptic conductance replaces the input from a presynaptic Purkinje cell. (**b**) After a 4-s-long baseline period (last 0.5 s is shown, gray), a train of 40 dynamic-clamp synaptic inputs (synaptic conductance, $g_{syn} = 1.5$ nS; synaptic reversal potential, $E_{rev} = 0$ mV, see Methods) were delivered at 5 Hz (first seven indicated by arrows), which led to the emergence of correlated activity and Purkinje cell entrainment (top, 20 overlaid sweeps; bottom, spike histogram; spike rate = 5.8 Hz). Sinusoid fits to the cross-correlograms (inset right, dashed lines; compare top and bottom) were used to assess the degree and phase of entrainment. Scale bars represent 10 mV (above) or 10 action potentials (APs; below), and 200 ms. (**c**) Switching on a similar, but hyperpolarizing, dynamic-clamp synapse ($g_{syn} = 1$ nS, $E_{rev} = -80$ mV, see Methods) in another Purkinje cell also entrained structured spiking (top, 20 overlaid sweeps; bottom, spike histogram; rate = 5.4 Hz) but with a different phase of the postsynaptic firing relative to the input (compare bottom right cross-correlogram with that in **b**). Scale bars represent 10 mV (above) or 10 APs (below), and 200 ms. (**d**) The amount of entrainment (**b**,**c**) was greatest for strongly hyperpolarizing and strongly depolarizing synaptic reversal potentials (blue, $E_{rev} < -50$ mV; red, otherwise). (**e**) The average phase (ϕ) of the entrainment was significantly different for hyperpolarizing and depolarizing synaptic reversal potentials ($P < 0.001$, $n = 9$ for hyperpolarizing synaptic potentials and $n = 10$ for depolarizing).

frequency was determined by the reversal potential, the firing rate was overall only weakly affected by turning on the dynamic clamp synapse[22] (change in frequency in all cases < 1 Hz; data not shown). Taken together, these results suggest that Purkinje-Purkinje connections can promote synchronization of Purkinje cells, with the phase of entrainment being dependent on the driving force at GABAergic synapses. For a given sign, however, the phase of entrainment was independent of the actual value of E_{GABA}.

Waves of activity in model Purkinje cell chains

The ability of the Purkinje-Purkinje synapse to produce entrainment of Purkinje cell spiking in combination with the asymmetric nature of the connectivity suggests that this synaptic connection may be involved in coordinating waves of activity in the Purkinje cell network. To investigate this possibility, we built a model network of 50 Purkinje cells, including the known set of active conductances in Purkinje cells[23]. The neurons were connected in a chain-like manner on the basis of the directional asymmetry that we observed (**Fig. 3a**,**b**); each neuron was connected with the following five neurons in the chain (**Fig. 5a**). The model Purkinje-Purkinje synapse was calibrated on the basis of data obtained from electrophysiological experiments (**Fig. 4**, **Supplementary Fig. 3** and **Supplementary Methods** online). Two synaptic reversal potentials were studied: one for depolarizing synapses ($E_{GABA} = -40$ mV) and one for hyperpolarizing synapses ($E_{GABA} = -80$ mV; see **Supplementary Fig. 1**).

The model network of connected Purkinje cells showed spontaneous propagation of waves of activity (**Fig. 5b**,**c**). When the connection was excitatory, the first cell in the network was leading, causing the waves to propagate from the tip of the lobule down into the cerebellum (**Fig. 5b** and **Supplementary Movie 2** online). For the hyperpolarizing case, the last cell led the wave, which propagated from the interior of the cerebellum toward the apex of the lobule (**Fig. 5c** and **Supplementary Movie 3** online). These computer simulations thus provide a proof of principle that the connection between Purkinje cells could be the substrate for propagating waves of activity along the sagittal plane in the cerebellum.

To quantify the propagation of the waves, we performed a two-dimensional Fourier transformation on Purkinje cell binary spike trains from the network model, resulting in an angular spectrum of the raster plot. This decomposed the network spike train into waves of a given direction and velocity, represented as one distinct point on the spatial versus temporal frequency axes. When unconnected, however, the network produced a band at the intrinsic firing frequencies of the cells without any distinct pattern on the spatial frequency axis (**Fig. 5d**). The occurrence of waves in the Purkinje cell network model was validated by the peaks at either side of the 0 mm^{-1} spatial frequency line for the depolarizing and hyperpolarizing connections (**Fig. 5e**,**f**). The velocity of the wave was obtained from this; in these examples, the waves traveled at ~30 mm s^{-1} for the depolarizing network and ~2 mm s^{-1} for the hyperpolarizing network. Note that in all cases, higher frequency harmonics were also visible. In addition to the angular spectrum decomposition approach described above, we calculated spike delay histograms to quantify the waves of activity that were generated by the network (**Supplementary Fig. 4** online), which provided further verification of these traveling waves.

Next, we assessed the robustness of the propagating waves, as they are unlikely to exist in the brain if they are not robust in the network model. The waves appeared across a wide range of parameter values (Methods and **Supplementary Fig. 5** online), including halved synaptic strength, reduced number of postsynaptic partners, sparse connectivity and increased firing rates. Changing the synaptic reversal potential to shunting inhibition, however, abolished the waves[22] (**Supplementary Fig. 5**). Although a switch from asymmetric to symmetric connectivity did not eliminate waves, it transformed them into standing waves of similar frequency (**Supplementary Fig. 5**). In

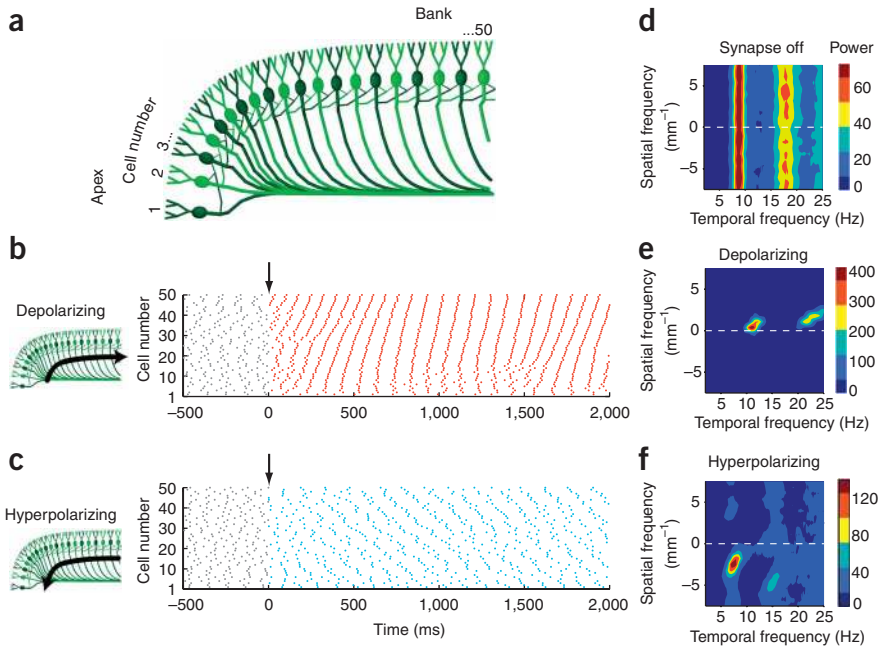

Figure 5 Waves of activity in a network model of Purkinje cells. (**a**) Schematic illustration of the Purkinje cell axon collateral network model (cells numbered starting at the apex of the folium). Each Purkinje cell was connected to the basally located nearest neighboring five cells (for illustrative purposes, only two connections are shown and cells have been colored in alternating colors). (**b**) Raster plot from the network model showing action potentials (individual dots) of Purkinje cells versus time (cells numbered as in **a**). Activation of depolarizing synapses (gray/red border, arrow) triggered waves of activity that traveled from the apex to the base of the folium (black arrow). (**c**) Activation of hyperpolarizing synapses (gray/blue border, arrow) triggered waves of activity that traveled in the opposite direction (black arrow). Note that the connectivity of the two networks in **b** and **c** was identical; only E_{GABA} differed. (**d**–**f**) Two-dimensional Fourier transformation contour plots corresponding to the angular spectrum of the raster plots. When the synapse was off (**d**), the two-dimensional Fourier transformation showed a flat band in the temporal frequency without structure in the spatial frequency dimension. In contrast, the two-dimensional Fourier transformation of the spike trains obtained with depolarizing (**e**) or hyperpolarizing connections (**f**) showed peaks that corresponded to traveling waves.

summary, the traveling waves are a robust phenomenon and are probably physiologically relevant.

Traveling waves in juvenile sagittal cerebellar slices

To test our model's prediction that waves of activity travel across Purkinje cells arranged in the sagittal plane of lobules, we recorded from Purkinje cells in sagittal slices from young mice (P4–6). We monitored Purkinje cell firing patterns non-invasively with extracellular recording electrodes. As basket and stellate cell inhibition is not yet established at this age[11], we were able to specifically isolate the effects of Purkinje cell synapses using $GABA_A$ receptor antagonists. Because the E_{GABA} that we found is depolarizing at these ages (**Supplementary Fig. 1**), our model predicted that waves of activity would travel from the apex toward the base of a cerebellar lobule (**Fig. 5b** and **Supplementary Movie 2**).

We used two-photon imaging to guide our electrodes to a region with intact axon collaterals and recorded activity from Purkinje cells lying in the same sagittal plane of the slice, typically two to three cell layers deep with a separation of 50–350 μm. Simultaneous extracellular recordings were made from two or three Purkinje cells (**Fig. 6a**,**b**). We looked for correlated activity between cells using a cross-correlation analysis of spike trains (**Fig. 6b**). Evidence for traveling waves of activity in Purkinje cells was determined by measuring the amplitude of a sine wave fit to the cross-correlogram; a bootstrap method was then employed to determine whether the cross-correlation was statistically significant (**Supplementary Methods**). Significant correlation was apparent in ~40% of paired extracellular recordings (17 of 41, $P \leq 0.05$). Considering that many of the axon collaterals are probably cut in the slice preparation, this ~40% occurrence of waves probably represents a lower bound and waves may be more prevalent in the intact brain. Notably, even at this young age, the asymmetric projection of collaterals was present ($n = 10$; data not shown). Similar to what has been observed in other brain regions during early development[24], cerebellar waves were intermittent, waxing and waning with time (**Supplementary Fig. 6** online).

To test whether the waves depend on GABAergic synapses (**Fig. 1c**), we applied the selective $GABA_A$ receptor antagonist SR95531. Perfusion of SR95531 significantly reduced the occurrence of correlated activity from ~40% in control conditions to ~5% of paired recordings (10 out of 25 in controls, 1 out of 15 during SR95531, $P = 0.012$; **Fig. 6b**,**c**), demonstrating that GABAergic synapses were critical for this form of correlated activity. Although Purkinje cell firing rates (6.1 ± 0.40 Hz, $n = 48$) were not altered by SR95531 (5.43 ± 0.40 Hz, $n = 28$, $P = 0.48$), one explanation for the absence of correlated firing in GABA blockade is that it arose indirectly as a result of an increase in the coefficient of variation of firing in individual Purkinje cells during SR95531 application. However, GABA blockade did not significantly regularize firing at these ages (coefficient of variation = 0.26 ± 0.04 for control and 0.35 ± 0.05 for SR95531, $P = 0.12$, $n = 28$). In addition, although peaky cross-correlograms were absent in SR95531, auto-correlograms for both pre- and postsynaptic firing were indistinguishable following this treatment (**Supplementary Fig. 6** and data not shown). These results demonstrate that the intrinsic firing of Purkinje cells was not altered by SR95531 at these ages. We conclude that $GABA_A$ receptors are important in the correlated firing of neighboring Purkinje cells. Given that SR95531 blocks traveling waves at a developmental time point at which other inhibitory inputs are not yet established[11], these results argue that the asymmetrically projecting connections between Purkinje cells are probably the key substrate for these waves.

We hypothesized that correlated firing between recorded cells arose because of waves of activity that travel along chains of Purkinje cells away from the apex of the lobule and toward its base. If this hypothesis was correct, the correlations between pairs of cells should depend on their spacing, as this would determine their relative position in the chain of connected Purkinje cells. To examine this possibility, we measured the phase difference, ϕ, between recorded cells (**Supplementary Methods**) and plotted it as a function of the number of Purkinje cells separating the electrodes. This produced a linear relationship: the phase difference was smaller for nearby cells and larger for more distant cells ($R = 0.82$, $P = 0.0001$; **Fig. 6d**), as predicted by the model when waves traveled away from the lobule apex. Furthermore, we found that waves moved at a speed of roughly 40 Purkinje cells per cycle, or ~3 mm s^{-1}, which was within the predicted range of the model. This

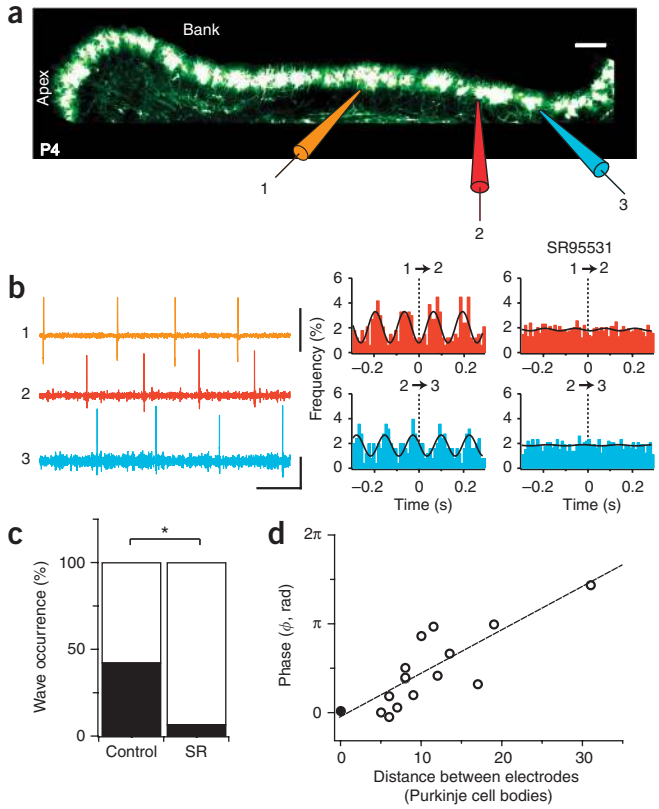

Figure 6 Traveling waves in sagittal cerebellar slices. (**a**) Cerebellar folium of a P4 *L7-tau-gfp* mouse illustrating the recording configuration in **b**. The positions of extracellular electrodes 1, 2 and 3 are indicated. Scale bar represents 50 μm. (**b**) Left, sample extracellular recording traces from electrodes in **a** showing waves of activity that traveled away from the lobule apex. Scale bars represent 1 nA (top trace), 100 pA (bottom two traces), and 100 ms. Right, cross-correlograms for pairs 1–2 and 2–3 indicated that firing was correlated. When SR95531 was perfused, the correlations were eliminated. (**c**) Summary data showing that the waves of activity that we observed in control conditions were abolished by SR95531. The perfusion of SR95531 (SR) significantly reduced the occurrence of wave-like activity between pairs of recordings from ~40% to ~5% (control waves, 10 out of 25 recordings; SR, 1 out of 15 recordings; * $P = 0.012$). (**d**) Waves traveled away from the lobule apex, as the phase (ϕ) of the sinusoid fit to the cross-correlograms between cells was significantly correlated with the number of somata separating recorded cells and the slope was positive ($R = 0.81$, $P = 0.0001$). The propagation velocity was ~40 Purkinje cells per period, or ~3 mm s^{-1}. The closed circle at zero distance shows the auto-correlogram data ($n = 4$).

lends further weight to our argument that the correlated firing arose from the Purkinje-Purkinje pathway, as this speed of propagation directly depends on the anatomical spacing of connected nodes in the chain of Purkinje cells.

To provide additional confirmation that the traveling waves were mediated by Purkinje axon collateral synapses, we carried out two-photon optical lesions of axon collaterals using a Ti:sapphire laser[25,26] or, in a subset of cases ($n = 2$), we lesioned with surgical scissors, providing an orthogonal approach to pharmacological blockade of the connection. To target the axon collateral connections, we took advantage of the laminar structure of the cerebellar cortex and carried out repeated scanning of the laser in a zone perpendicular to the Purkinje cell layer across visualized axon collaterals (**Fig. 7**). This approach enabled us to locally sever the majority of Purkinje cell axon collaterals. The tissue around the optical lesion appeared to be healthy both during and after the procedure (examined afterwards for up to 2 h). The morphology of Purkinje cells on either side of the lesion appeared to be normal (**Fig. 7a,b**) and Purkinje cell firing rates were unaffected (6.61 ± 0.34 Hz, before the optical lesion, $n = 34$; 6.03 ± 0.37 Hz after, $n = 36$; $P = 0.25$).

The two-photon optical lesion abolished traveling waves of activity in Purkinje cells across the lesion. In some cases, we were able to maintain continuous extracellular recordings from Purkinje cells on either side of the lesion (**Fig. 7a,b**). In control experiments, waves of activity were observed in ~40% of recordings made in the same, but unlesioned, tissue (7 out of 17 recordings). These were performed either before cutting (**Fig. 7a**) or 'upstream' of the cut, on the side closest to the lobule apex. When the Purkinje cell axon collaterals were

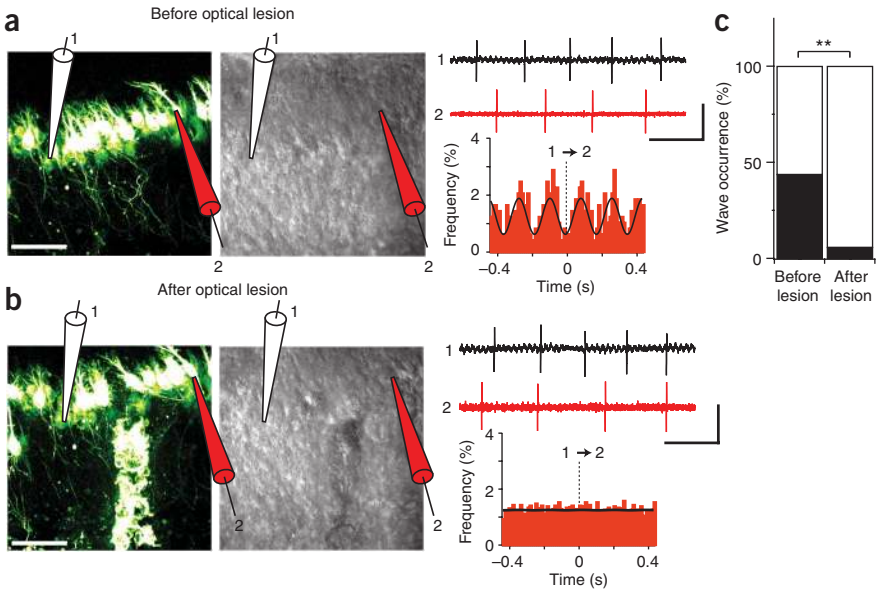

Figure 7 Optical lesion of Purkinje axon collaterals abolishes traveling waves. (**a**) Left, two-photon image (left) and corresponding laser-scanning Dodt contrast image (right) of *L7-tau-gfp* Purkinje cells from a P6 mouse illustrating the recording configuration, with the position of extracellular electrodes 1 and 2 shown. Scale bar represents 50 μm. Top right, sample traces from electrodes in **a** showing wave-like activity. Scale bars represent 200 pA (top trace), 500 pA (bottom trace) and 200 ms. Bottom right, peaks in cross-correlograms indicated that firing was correlated. (**b**) Images showing same location as **a** after optical lesioning of collaterals in the granule cell layer. The lesion appeared both as a bright fluorescent band (left) and a faint scar (middle). Scale bar represents 50 μm. Top right, sample traces from the same cells after the optical lesion, when wave-like activity is abolished. Scale bars represent 500 pA (top trace), 750 pA (bottom trace) and 200 ms. Bottom right, absence of peaks in cross-correlogram after optical lesioning. (**c**) Waves were seldom observed in Purkinje cells following optical lesioning of axon collaterals. For control data in the same slice, waves were seen at the same rates as were seen previously, ~40% (7 out of 17 recordings). However, across the lesion, waves were seen significantly less often (1 out of 18 recordings, ** $P = 0.0047$).

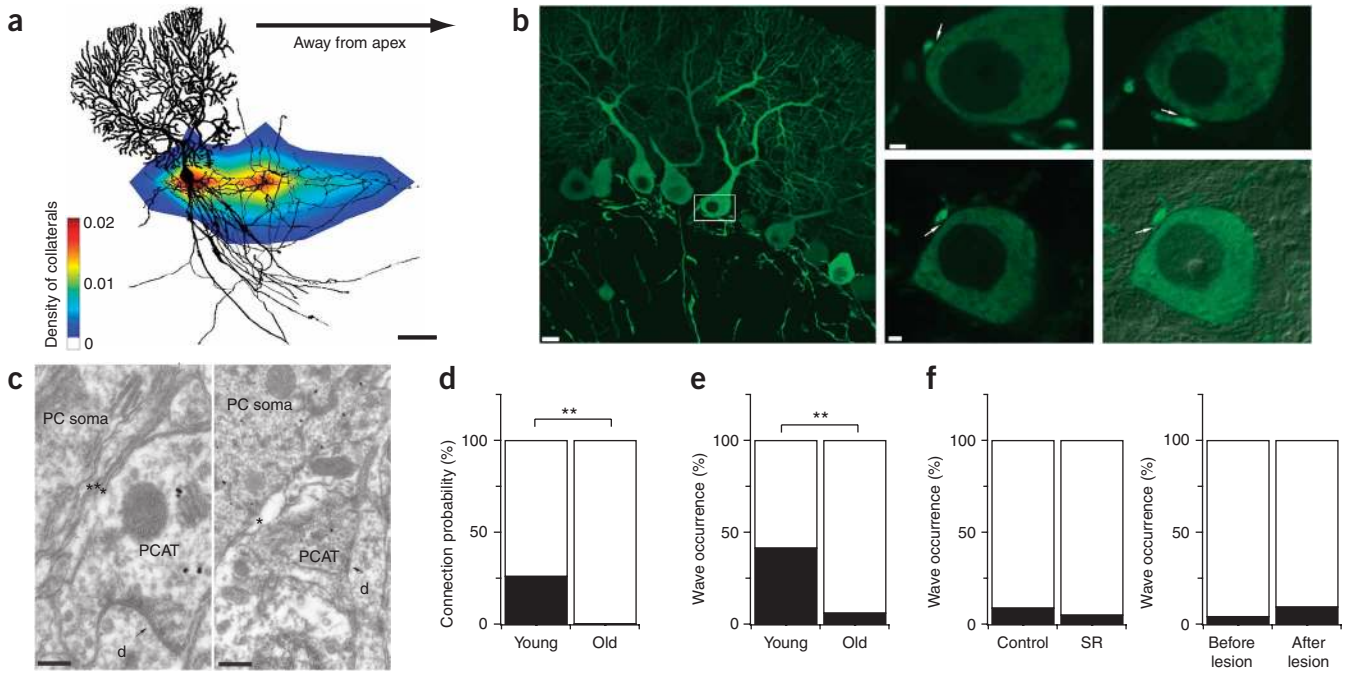

Figure 8 Purkinje cell-Purkinje cell connectivity and traveling waves are absent in older mice. (**a**) Density plot of Purkinje cell axon collaterals from older mice revealed that collaterals projected asymmetrically away from lobule apex ($n = 14$, P17–22; see **Fig. 3b** and Methods). Scale bar represents 50 μm. (**b**) Left, confocal image from a P18 mouse. Scale bar represents 10 μm. Right, high-magnification single optical section images from the boxed area. Arrows point to gaps between Purkinje cell axon terminals and the soma. Scale bars represent 2 μm. (**c**) Electron micrographs showing that Purkinje cell axon terminals were close to, but did not form synapses with, Purkinje cell somata. Often, thin layers of membrane (left, asterisks) or a gap (right, asterisk) separated the structures. Purkinje cell axon terminals established a synaptic junction (arrows) with nonlabeled, non–Purkinje cell dendrites (d). Scale bars represent 0.2 μm (left) and 0.5 μm (right). (**d**) The connectivity rate of monosynaptic Purkinje-Purkinje cell connections was significantly reduced in older mice (P4–14, 23 of 88 tested connections; P17–25, 0 of 25 tested connections; ** $P < 0.001$). (**e**) The occurrence of waves was reduced in older mice to chance levels (P4–6, 17 out of 41 pairs of recordings; P17–25, 5 out of 81; ** $P < 0.001$). (**f**) Neither SR95531 (left; matched control, 3 out of 34 pairs of recordings; SR, 1 out of 20 recordings; $P = 0.31$) nor optical lesioning of Purkinje cell collaterals (right; before lesion, 2 out of 48 recordings; after lesion, 3 out of 32 recordings; $P = 0.18$) affected waves in older mice.

ablated, cross-correlations were observed in only 1 out of 18 recordings, which was a significant reduction from control conditions ($P = 0.0047$; **Fig. 7b,c**). The occasional presence of correlated activity across an optical lesion was not surprising, as the full depth of the slice could not readily be cut with the laser. Given that optical lesioning abolished correlated activity between pairs of Purkinje cells spanning the lesion, but not between pairs of Purkinje cells located distal to the lesion, these data suggest that the ablated axon collaterals were the critical substrate for these traveling waves. Taken together, our data provide strong evidence in favor of the view that the Purkinje-Purkinje cell axon collateral pathway is the substrate for traveling waves of activity in chains of connected Purkinje cells in the juvenile cerebellar cortex.

Traveling waves are ontogenetically transient

Although many Purkinje cell axon collaterals are pruned during development, at least some Purkinje cells retain some of their local axon collaterals[10]. We investigated whether traveling waves were still present in older mice. Because traveling waves critically depend on the asymmetrical projection pattern of Purkinje cell axon collaterals, we first asked whether this persists in older mice. Although subtle differences in the axonal projection pattern may emerge during development, the general asymmetrical projection motif that we found in juveniles (**Fig. 3b**) was maintained in older mice (P17–24, $n = 14$; **Fig. 8a**). This suggested that Purkinje cell axon collaterals might maintain their capacity to generate traveling waves in the mature brain.

We next asked whether Purkinje cell axon collaterals made monosynaptic connections with other Purkinje cells in older mice. To address this question, we first examined the target of these collaterals in P18 mice at both light microscopic and electron microscopic levels. To our surprise, confocal imaging showed that although Purkinje cell axon collaterals entered the Purkinje cell layer, they appeared very close to, but not directly apposed to, nearby Purkinje cell somata (**Fig. 8b**; compare with **Fig. 2a–d**). A small gap between the presynaptic bouton and Purkinje cell soma was discernable in most cases (**Fig. 8b**). Our results suggest that these collaterals no longer directly target Purkinje cells in older mice. To further address this possibility, we next examined the target of Purkinje cell axon collaterals at the ultrastructural level. To visualize Purkinje cell axon terminals, we performed immunogold reactions to GFP. Our electron microscopic analysis revealed that although Purkinje cell axon collaterals were found within a few hundred nanometer of Purkinje cell somata (**Fig. 8c**), they did not form synapses on them. Between Purkinje cell axons and somata we typically found thin layers of presumed glial membrane (**Fig. 8c**). In addition, we could not find any presynaptic specializations or postsynaptic densities at these appositions, thus suggesting the absence of functional Purkinje-Purkinje cell synapses. However, Purkinje cell axon terminals did form synapses onto nearby dendrites of unlabeled non-Purkinje cells (**Fig. 8c**), perhaps arising from basket cells[27], which argues that the examined Purkinje cell axons were indeed fully functional and were able to form synapses.

To investigate further the existence of monosynaptic Purkinje-Purkinje cell connections in relatively mature mice, we carried out targeted paired recordings as described earlier. Consistent with our light microscopic and electron microscopic results, we found no

monosynaptically connected Purkinje cell pairs in 3-week-old mice (P17–25, 0 pairs out of 25 tested; P4–14, 23 pairs out of 88 tested; significantly different, $P = 0.002$; **Fig. 8d**). Although we cannot rule out the existence of sparse Purkinje-Purkinje synapses in older mice, our results suggest that the Purkinje-Purkinje pathway is pruned following postnatal development and that Purkinje cells are not the main target of Purkinje cell local axon collaterals in adult mice.

We next investigated whether traveling waves of activity exist in sagittal slices from older mice using the same methods that we employed in young mice. Although correlated activity was sometimes observed and at times appeared to be quite strong, bootstrap analysis showed that these correlations were usually not statistically significant ($P > 0.05$), but were instead spurious, arising as a result of the much more regular firing and overall higher firing frequencies of mature Purkinje cells[28,29]. Indeed, significantly correlated activity was rarely observed in older mice and significantly less often than in young mice (young, 17 of 41 recordings; old, 5 of 81; $P < 0.0001$; **Fig. 8e**). Finally, the occasional incidence of correlated activity in mature cerebellar cortex was not significantly altered following the blockade of $GABA_A$ receptors (SR95531: 1 of 20 recordings; control: 3 of 34; $P = 0.31$; **Fig. 8f**) nor by optical lesioning of Purkinje cell axons (before lesion: 2 of 46 recordings; after: 3 of 32; $P = 0.18$; **Fig. 8f**), again suggesting that the rare occurrence of cross-correlations in older mice was spurious in nature and not mediated by Purkinje axon signaling.

Taken together, our anatomical, electrophysiological and modeling results suggest that Purkinje-Purkinje cell monosynaptic connections are the substrate of traveling waves in juvenile mice. The fact that we did not find direct monosynaptic connections or substantial traveling waves in older mice adds weight to our conclusion that the Purkinje-Purkinje pathway underpins these waves. Furthermore, the observation that these traveling waves are ontogenetically transient suggests that they may be important in the development of the cerebellar circuit.

DISCUSSION

We provide anatomical and physiological evidence that Purkinje cells are monosynaptically connected via GABAergic synapses in juvenile mice. These Purkinje-Purkinje synapses have either a potent excitatory or inhibitory effect on postsynaptic spiking, depending on E_{GABA} and developmental stage. The connection shows a marked asymmetry along the sagittal axis of a cerebellar folium. A realistic model that is based on the experimentally determined parameters demonstrates that this connection can mediate traveling waves of activity in the cerebellar cortex. We tested this model, directly demonstrated for the first time, to the best of our knowledge, the presence of waves of activity in juvenile sagittal cerebellum, and used pharmacological blockers and optical lesions to show that these waves arise predominantly from Purkinje cell local axon collaterals. These waves are ontogenetically transient, as they were not observed in more mature slices, in which our anatomical and physiological results indicate that the majority of monosynaptic connections between Purkinje cells have been pruned. This is consistent with some previous reports[5,6], although others have found evidence for Purkinje-Purkinje synapses in adults[2,4]; however, the criteria for identifying Purkinje cell axons in these studies were not as specific as the immuno–electron microscopic labeling that we used. As the proper development of mature circuits in other juvenile brain regions is known to be critically dependent on early and ontogenetically transient wave activity[12–14], we suggest that waves of activity that travel along chains of connected Purkinje cells in immature cerebellum may have a similar role in cerebellar development.

An asymmetric synaptic connection between Purkinje cells

Our combined anatomical and physiological results indicate that the Purkinje-Purkinje synapses represent an important feature of the connectivity of the developing cerebellar cortex. Nearly one third of pairs of neighboring Purkinje cells in the sagittal plane formed functional connections, as shown by targeted recordings. Purkinje cell collaterals can extend to more than 200 μm from the parent soma (**Fig. 3b**, and see refs. 2,27,30 for examples), indicating that a single Purkinje cell could target as many as ten neighboring Purkinje cells, although most of our functional connections were made within 100 μm of the parent soma. The connectivity rate was developmentally regulated. It was highest in young mice and appeared to decrease during the second postnatal week[7], and by the third postnatal week, functional synaptic connections were very sparse or even absent (**Fig. 8**). This finding may explain why functional connectivity among Purkinje cells was not observed in many previous slice experiments.

We found that a defining feature of this synaptic connection was a marked asymmetry in the projection of the Purkinje cell axon collateral, which showed a strong preference to follow the direction of projection of the main axon in the sagittal plane. This was predominantly away from the apex of the folium and toward the white matter and the DCN at the center of the cerebellum. We did not observe reciprocal connections between Purkinje cells, in stark contrast with the neocortex, where circular and reciprocal connectivity motifs among neighboring pyramidal neurons are common[31]. This asymmetry should also hold for any functional connections made by the Purkinje cell collaterals with other potential targets in the cerebellar cortex, such as GABAergic interneurons[27]. It will be interesting to determine the molecular and cellular mechanisms that are responsible for establishing and maintaining this directionality, particularly as there is evidence for some pruning of axon collaterals during development[10] and the collaterals appear to respect the zebrin compartmentalization of the cerebellar cortex[30].

Strength and synaptic dynamics of the connection

We found that the synaptic connection between Purkinje cells was mediated by activation of $GABA_A$ receptors, indicating that the same transmitter was released from the Purkinje cell collaterals as is released by synapses made by the main Purkinje cell axons in the DCN[32,33]. Our dynamic clamp data indicate that unitary Purkinje-Purkinje synapses can have a substantial effect on the spiking of postsynaptic Purkinje cells, either by delaying or advancing spontaneous spikes, depending on the reversal potential. This is comparable to the effect of basket and stellate cell connections with Purkinje cells, where unitary inputs can also substantially inhibit Purkinje cell spiking[19,34]. Given that basket and stellate cell inputs do not appear until the second postnatal week[11], this indicates that the Purkinje-Purkinje synapses may have a dominant effect on excitability in the first postnatal week, which is further ensured by the axosomatic location of their synaptic contacts. Notably, the basket/stellate cell connections with Purkinje cells undergo a marked 11-fold weakening during development (from P11 to P31)[35]. There does not seem to be a similar downregulation of cell mean synaptic conductance over the age range that we studied (see also ref. 7), although there appeared to be a marked reduction in the connectivity rate, with the majority of Purkinje-Purkinje synapses being pruned by the third postnatal week (**Fig. 8**).

Early in development, the Purkinje-Purkinje cell synapse shows robust short-term depression over a wide range of presynaptic firing rates. Following the second postnatal week, however, the synaptic dynamics eventually become facilitating (also see ref. 7). A similar change in synaptic dynamics during development has also been shown

at other synaptic connections[36], including at other inhibitory synapses onto Purkinje cells[35]. Because Purkinje cells are spontaneously active[18,19], even at young ages, these synapses are probably tonically depressed over the normal range of Purkinje cell firing in young mice, particularly during the first postnatal week of development, when the synaptic reversal potential was depolarizing and short-term depression was strongest (**Supplementary Fig. 1**). This implies that in young animals, paradoxically, a pause in Purkinje cell spiking may release the synapse from this tonically depressed state[32,33], producing an enhanced synaptic conductance.

Traveling waves of activity in cerebellar cortex

Although traveling waves of activity are crucial early on for proper circuit development in several CNS regions[12–14], this pattern of activity has, to the best of our knowledge, not yet been described in the developing cerebellum. The mechanisms controlling early waves in other brain regions are diverse and can vary throughout development[24]. However, depolarizing GABAergic transmission early in development appears to be important for the production of waves in several circuits[37], which is consistent with our findings in the cerebellum.

The cerebellar cortex has been thought to lack recurrent excitatory feedback, as the only intrinsic glutamatergic connections (made by granule cells and unipolar brush cells) are strictly feedforward. Our finding of functional connections between Purkinje cells, coupled with the demonstration that these connections can be excitatory early in development, provides a new pathway for recurrent local excitation. This pathway has some marked differences from excitatory feedback connections in cortical circuits, which have been proposed to serve many functional roles, from gain control, signal restoration, input selection, information storage and working memory, through to their role in pathological states such as epilepsy[38,39]. First, the excitation in the Purkinje cell recurrent network is ontogenetically transient, as it switches to inhibition later in development and is eventually pruned. Second, the projection is directional; Purkinje cells tend to project in only one direction along the sagittal axis and reciprocal connections are therefore rare. Consequently, this connection is unlikely to sustain positive feedback and reverberant activity, as in cortical circuits, because the network lacks the mutual reinforcement required for this to occur.

Our simple model of the Purkinje cell network, constrained by our functional and anatomical data, generated traveling waves of activity in the Purkinje cell population, the direction and speed of which depend on the GABAergic reversal potential. We directly validated our model by demonstrating the existence of traveling waves of activity in juvenile Purkinje cells in sagittal slices. Traveling waves have previously been shown to be an emergent property in network models (for example, see ref. 40). However, our model is the first to show, to the best of our knowledge, waves of activity that rely on a known anatomical asymmetry in a single type of synaptic connection constrained directly by experimental data and thus differs from previous models showing that Purkinje cell collaterals can promote synchrony in the form of standing waves or oscillations in the Purkinje cell population[8,41]. The anatomical origin of the waves (together with the kinetics of the synaptic connection and the spontaneous firing of the Purkinje cells) helps to account for the different network dynamics in the Purkinje cell network compared with more conventional recurrent feedback-based excitatory and inhibitory network models, which exhibit synchrony, but no clear waves[22,42]. It will be interesting to determine whether anatomical asymmetries in axonal projections found in other brain regions can also support waves and the extent to which waves documented experimentally in other brain areas (for example, see ref. 43) are linked to possible asymmetries in axonal projections.

Functional implications of traveling waves

What makes traveling waves different from other forms of oscillatory activity? Although theoretical and experimental evidence for oscillatory activity in the form of standing waves in the cerebellar cortex is abundant (for a review, see ref. 44), our data represent, to the best of our knowledge, the first evidence for traveling waves in the cerebellar cortex. Traveling waves are not incompatible with oscillatory activity in the form of standing waves. Indeed, traveling waves might appear to be standing waves if the particular spatial properties of the wave are not captured in the recording configuration. It is also possible that both forms of activity may coexist, as both high-frequency standing wave oscillations and lower-frequency traveling waves can arise from a population of spiking neurons. However, traveling waves are different from standing waves in that they propagate information across neuronal tissue; thus, the former contain directional information in addition to the temporal and spatial information that is contained in both types of waves. During development, traveling waves may therefore be important in the formation of functional maps and local subnetworks. Indeed, a recent study in cat visual cortex[45] found that traveling waves were essential for a computational model to predict how synaptic plasticity rewires cortical maps after injury. In the same model, standing wave oscillatory activity, however, lead to incorrectly predicted remapping[45]. Recent work in the retina demonstrated the existence of two temporally and mechanistically distinct forms of waves: standing waves in early development and traveling waves later in development. Furthermore, these later traveling waves are required to ensure the proper formation of the ON and OFF subnetworks in the retina[46].

What is the functional role of these sagittal waves of activity in the developing Purkinje cell population? These waves could represent the sagittal counterpart of the activity patterns that are postulated to spread along the 'beam' of active parallel fibers[47,48]; the ordered propagation of the waves could provide a timing signal that is important for activating Purkinje cells associated with different components of a movement sequence. This in effect forms a functional compartment in the developing cerebellar cortex, whereby each lobule supports two traveling waves that move along opposite lobule banks (**Supplementary Fig. 7** online). One possibility is that the compartmentalization of the cerebellar cortex in the sagittal domain, which may include zebrin-expressing Purkinje cell clusters[30] and the extent of sagittal spread of climbing fiber collaterals[49], is partly governed by sagittal waves, together with appropriate activity-dependent synaptic plasticity learning rules.

Another possible and not mutually exclusive function of these early waves may be that they are involved in establishing the proper pattern of synaptic connectivity of Purkinje cell inputs to the DCN. Indeed, the effect of the waves of activity on the downstream neurons in the DCN will depend on the detailed pattern of synaptic connectivity: that is, how the cerebellar folium is mapped onto individual DCN neurons, which is currently poorly understood. If input from Purkinje cells along a folium is represented topographically in the DCN, these waves may be involved in the normal wiring of the DCN. Such a wiring strategy might permit directionally dependent dendritic computation[50], which would be sensitive to different directions of propagation of the waves in cerebellar cortex. In many brain regions, early spontaneous waves precede sensory input and are thought to provide a critical substrate in the organization of neuronal circuitry, which is further refined later in development by sensory input. We suggest that traveling waves could thus represent a cerebellar analog of these self-organizing, presensory input circuit mechanisms. Further investigations of these waves are required to gain a better understanding of their functional roles during the development of the cerebellar circuit.

METHODS

Experiments. All experiments were carried out in accordance with the animal care and handling guidelines approved by the UK Home Office. Acute cerebellar slices were prepared from P3–25 *L7-tau-gfp* mice[15] or, in a few cases, *Gad65-egfp* mice[16,17] using standard techniques[19]. All electrophysiological experiments were carried out at 33–35 °C. For confocal and electron microscopy, *L7-tau-gfp* mouse pups (P8 or P18) were transcardially perfused with fixative before we carried out immunohistochemical and immmunogold labeling. For further details, see the **Supplementary Methods**.

Network modeling. A network simulation consisting of 50 synaptically connected Purkinje cells was implemented in NEURON (http://www.neuron.yale.edu/) using a biophysical model of the Purkinje cell based on an existing model for spontaneously firing Purkinje cells[23]. The anatomical and physiological parameters of the model were tuned to replicate our experimental data. Further details are available in the **Supplementary Methods**.

Data analysis and statistics. Data are reported as means ± s.e.m. unless otherwise indicated. Data analysis was performed using Igor Pro (Wavemetrics) and Matlab (MathWorks). Comparisons were made using either paired two-tailed Student's *t* tests or unpaired two-tailed Student's *t* tests, assuming unequal variances. Further details are available in the **Supplementary Methods**.

Note: Supplementary information is available on the Nature Neuroscience website.

ACKNOWLEDGMENTS

We thank B. Clark, I. Duguid, F. Edwards, S. Ho, T. Ishikawa, M. London, E. Rancz, A. Roth and S. Smith for helpful discussions and for comments on the manuscript. We are grateful to S. du Lac, G. Szabó and F. Erdélyi for providing transgenic mice, to J. Gruendemann for providing tissue for reconstructions, to B. Clark for help with perfusions, and to L. Ramakrishnan and K. Powell for expert assistance with histology and Neurolucida reconstructions. This work was funded by a European Molecular Biology Organization Long-Term Fellowship and a Royal Society Dorothy Hodgkin Fellowship to A.J.W., a Feodor Lynen Fellowship of the Alexander von Humboldt Foundation to H.C., a European Young Investigator Award and a Wellcome Trust project grant to Z.N., a Marie-Curie Intra-European fellowship and Medical Research Council Career Development Award to P.J.S., and a Wellcome Trust Senior Research Fellowship and a grant from the Gatsby Foundation to M.H.

Published online at http://www.nature.com/natureneuroscience/
Reprints and permissions information is available online at http://www.nature.com/reprintsandpermissions/

1. Ivry, R. Cerebellar timing systems. *Int. Rev. Neurobiol.* **41**, 555–573 (1997).
2. Chan-Palay, V. The recurrent collaterals of Purkinje cell axons: a correlated study of the rat's cerebellar cortex with electron microscopy and the Golgi method. *Z. Anat. Entwicklungsgesch.* **134**, 200–234 (1971).
3. Ramon y Cajal, S. *Histologie du Systeme Nerveux de l'homme et des Vertebres* (Maloine, Paris, 1911).
4. Larramendi, L.M. & Lemkey-Johnston, N. The distribution of recurrent Purkinje collateral synapses in the mouse cerebellar cortex: an electron microscopic study. *J. Comp. Neurol.* **138**, 451–459 (1970).
5. Hamori, J. & Szentagothai, J. Identification of synapses formed in the cerebellar cortex by Purkinje axon collaterals: an electron microscope study. *Exp. Brain Res.* **5**, 118–128 (1968).
6. De Camilli, P., Miller, P.E., Levitt, P., Walter, U. & Greengard, P. Anatomy of cerebellar Purkinje cells in the rat determined by a specific immunohistochemical marker. *Neuroscience* **11**, 761–817 (1984).
7. Orduz, D. & Llano, I. Recurrent axon collaterals underlie facilitating synapses between cerebellar Purkinje cells. *Proc. Natl. Acad. Sci. USA* **104**, 17831–17836 (2007).
8. Maex, R. & De Schutter, E. Oscillations in the cerebellar cortex: a prediction of their frequency bands. *Prog. Brain Res.* **148**, 181–188 (2005).
9. Sotelo, C. Cellular and genetic regulation of the development of the cerebellar system. *Prog. Neurobiol.* **72**, 295–339 (2004).
10. Gianola, S., Savio, T., Schwab, M.E. & Rossi, F. Cell-autonomous mechanisms and myelin-associated factors contribute to the development of Purkinje axon intracortical plexus in the rat cerebellum. *J. Neurosci.* **23**, 4613–4624 (2003).
11. Altman, J. Postnatal development of the cerebellar cortex in the rat. II. Phases in the maturation of Purkinje cells and of the molecular layer. *J. Comp. Neurol.* **145**, 399–463 (1972).
12. Feller, M.B. Spontaneous correlated activity in developing neural circuits. *Neuron* **22**, 653–656 (1999).
13. Ben-Ari, Y. Developing networks play a similar melody. *Trends Neurosci.* **24**, 353–360 (2001).
14. Katz, L.C. & Shatz, C.J. Synaptic activity and the construction of cortical circuits. *Science* **274**, 1133–1138 (1996).
15. Sekirnjak, C., Vissel, B., Bollinger, J., Faulstich, M. & du Lac, S. Purkinje cell synapses target physiologically unique brainstem neurons. *J. Neurosci.* **23**, 6392–6398 (2003).
16. Bali, B., Erdélyi, F., Szabó, G. & Kovacs, K.J. Visualization of stress-responsive inhibitory circuits in the GAD65-eGFP transgenic mice. *Neurosci. Lett.* **380**, 60–65 (2005).
17. Erdélyi, F. *et al.* GAD65-GFP transgenic mice expressing GFP in the GABAergic nervous system. *FENS Abstr.* **1**, A011.3 (2003).
18. Raman, I.M. & Bean, B.P. Resurgent sodium current and action potential formation in dissociated cerebellar Purkinje neurons. *J. Neurosci.* **17**, 4517–4526 (1997).
19. Häusser, M. & Clark, B.A. Tonic synaptic inhibition modulates neuronal output pattern and spatiotemporal synaptic integration. *Neuron* **19**, 665–678 (1997).
20. Mittmann, W. & Häusser, M. Linking synaptic plasticity and spike output at excitatory and inhibitory synapses onto cerebellar Purkinje cells. *J. Neurosci.* **27**, 5559–5570 (2007).
21. Eilers, J., Plant, T.D., Marandi, N. & Konnerth, A. GABA-mediated Ca^{2+} signaling in developing rat cerebellar Purkinje neurones. *J. Physiol. (Lond.)* **536**, 429–437 (2001).
22. Vida, I., Bartos, M. & Jonas, P. Shunting inhibition improves robustness of gamma oscillations in hippocampal interneuron networks by homogenizing firing rates. *Neuron* **49**, 107–117 (2006).
23. Khaliq, Z.M., Gouwens, N.W. & Raman, I.M. The contribution of resurgent sodium current to high-frequency firing in Purkinje neurons: an experimental and modeling study. *J. Neurosci.* **23**, 4899–4912 (2003).
24. Firth, S.I., Wang, C.T. & Feller, M.B. Retinal waves: mechanisms and function in visual system development. *Cell Calcium* **37**, 425–432 (2005).
25. Yanik, M.F. *et al.* Neurosurgery: functional regeneration after laser axotomy. *Nature* **432**, 822 (2004).
26. Mejia-Gervacio, S. *et al.* Axonal speeding: shaping synaptic potentials in small neurons by the axonal membrane compartment. *Neuron* **53**, 843–855 (2007).
27. O'Donoghue, D.L., King, J.S. & Bishop, G.A. Physiological and anatomical studies of the interactions between Purkinje cells and basket cells in the cat's cerebellar cortex: evidence for a unitary relationship. *J. Neurosci.* **9**, 2141–2150 (1989).
28. Brody, C.D. Correlations without synchrony. *Neural Comput.* **11**, 1537–1551 (1999).
29. de la Rocha, J., Doiron, B., Shea-Brown, E., Josic, K. & Reyes, A. Correlation between neural spike trains increases with firing rate. *Nature* **448**, 802–806 (2007).
30. Hawkes, R. & Leclerc, N. Purkinje cell axon collateral distributions reflect the chemical compartmentation of the rat cerebellar cortex. *Brain Res.* **476**, 279–290 (1989).
31. Song, S., Sjöstrom, P.J., Reigl, M., Nelson, S. & Chklovskii, D.B. Highly nonrandom features of synaptic connectivity in local cortical circuits. *PLoS Biol.* **3**, e68 (2005).
32. Pedroarena, C.M. & Schwarz, C. Efficacy and short-term plasticity at GABAergic synapses between Purkinje and cerebellar nuclei neurons. *J. Neurophysiol.* **89**, 704–715 (2003).
33. Telgkamp, P. & Raman, I.M. Depression of inhibitory synaptic transmission between Purkinje cells and neurons of the cerebellar nuclei. *J. Neurosci.* **22**, 8447–8457 (2002).
34. Midtgaard, J. Stellate cell inhibition of Purkinje cells in the turtle cerebellum *in vitro*. *J. Physiol. (Lond.)* **457**, 355–367 (1992).
35. Pouzat, C. & Hestrin, S. Developmental regulation of basket/stellate cell→Purkinje cell synapses in the cerebellum. *J. Neurosci.* **17**, 9104–9112 (1997).
36. Reyes, A. & Sakmann, B. Developmental switch in the short-term modification of unitary EPSPs evoked in layer 2/3 and layer 5 pyramidal neurons of rat neocortex. *J. Neurosci.* **19**, 3827–3835 (1999).
37. Ben-Ari, Y. Excitatory actions of gaba during development: the nature of the nurture. *Nat. Rev. Neurosci.* **3**, 728–739 (2002).
38. Douglas, R.J. & Martin, K.A. Recurrent neuronal circuits in the neocortex. *Curr. Biol.* **17**, R496–R500 (2007).
39. Connors, B.W. & Telfeian, A.E. Dynamic properties of cells, synapses, circuits and seizures in neocortex. *Adv. Neurol.* **84**, 141–152 (2000).
40. Cohen, A.H. *et al.* Modelling of intersegmental coordination in the lamprey central pattern generator for locomotion. *Trends Neurosci.* **15**, 434–438 (1992).
41. de Solages, C. *et al.* High-frequency organization and synchrony of activity in the purkinje cell layer of the cerebellum. *Neuron* **58**, 775–788 (2008).
42. Geisler, C., Brunel, N. & Wang, X.J. Contributions of intrinsic membrane dynamics to fast network oscillations with irregular neuronal discharges. *J. Neurophysiol.* **94**, 4344–4361 (2005).
43. Lee, S.H., Blake, R. & Heeger, D.J. Traveling waves of activity in primary visual cortex during binocular rivalry. *Nat. Neurosci.* **8**, 22–23 (2005).
44. De Zeeuw, C.I., Hoebeek, F.E. & Schonewille, M. Causes and consequences of oscillations in the cerebellar cortex. *Neuron* **58**, 655–658 (2008).
45. Young, J.M. *et al.* Cortical reorganization consistent with spike timing, but not correlation, dependent plasticity. *Nat. Neurosci.* **10**, 887–895 (2007).
46. Kerschensteiner, D. & Wong, R.O. A precisely timed asynchronous pattern of ON and OFF retinal ganglion cell activity during propagation of retinal waves. *Neuron* **58**, 851–858 (2008).
47. Braitenberg, V. Functional interpretation of cerebellar histology. *Nature* **190**, 539–540 (1961).
48. Eccles, J.C., Szentagothai, J. & Ito, M. *The Cerebellum as a Neuronal Machine* (Springer-Verlag, Heidelberg, 1967).
49. Oberdick, J., Baader, S.L. & Schilling, K. From zebra stripes to postal zones: deciphering patterns of gene expression in the cerebellum. *Trends Neurosci.* **21**, 383–390 (1998).
50. Rall, W. Theoretical significance of dendritic trees for neuronal input-output relations. in *Neural Theory and Modeling* (ed. Reiss, R.F. 73–97 (Stanford University Press, Stanford, California, USA, 1964).